ELSEVIER

0140-7007(95)00082-8

Int J. Refrig. Vol. 19, No. 2, pp. 107–114, 1996

0140-7007/96/$15.00

A simple method for prediction of chilling times: extension to three-dimensional irregular shapes

Zhang Lin, A. C. Cleland, D. J. Cleland and G. F. Serrallach
Massey University, Private Bag 11-222, Palmerston North, New Zealand

The extension of a previously published empirical chilling time prediction method to three-dimensional irregular shapes was investigated. The real geometric shapes were related to equivalent ellipsoids using simple geometric measurements. Chilling time estimates were made using two shape-dependent parameters in conjunction with the first term in the series-analytical solution for convective cooling of a sphere. Experiments for eight geometric shapes (21 runs) were used to validate the model for thermal centre temperature predictions. The accuracy of the model for predicting mass-average temperatures of irregular shapes was not tested. Accurate chilling time prediction by a method employing only simple algebraic expressions is now possible for objects of any shape.
(Keywords: chilling; chilling time; simulation; calculation; measurement)

Methode simple de prevision des durees de refrigeration: application a des formes irregulieres tri-dimensionnelles

On a étudié l'application d'une méthode de prévision des durées de réfrigération empirique, publiée antérieurement, à des formes irrégulières tri-dimensionnelles. On a associé les formes géométriques réelles à des ellipsoïdes équivalents utilisant des mesures géométriques simples. On a estimé les durées de réfrigération en utilisant deux paramètres dépendant de la forme ainsi que le premier terme dans la résolution analytique de série se rapportant au refroidissement par convection d'une sphère. Les expériences menées sur 8 formes géometriques (21 essais) ont été utilisées pour valider le modèle de prévision de la température centrale thermique. On n'a pas essayé la précision du modèle pour la prévision des températures moyennes des formes irrégulières. Il est à présent possible de prévoir précisément la durée de réfrigération d'objets de n'importe quelle forme, grâce à une méthode employant seulement des expressions algébriques simples.
(Mot clés: réfrigération; temps de réfrigération; simulation; calcul; mesure)

Many foods that are chilled industrially are of three-dimensional irregular shape, e.g. fruit and vegetables, fish, poultry, meat carcasses and commercial cuts of meat. Therefore accurate prediction of chilling times for products of three-dimensional irregular shape is important for the design of food chilling operations.

In previous papers[1,2], a simple method for chilling time prediction was proposed. It involves use of the first term of the analytical series solution for convective cooling of a sphere[3] in conjunction with two shape-dependent parameters designated E and L. Empirical algebraic equations for E and L, which apply to regular multidimensional objects (infinite rectangular rods, rectangular bricks and finite cylinders) and elliptical two-dimensional objects, were presented. The resulting prediction method has the form:

$$Y = L\exp\left(-E\alpha^2\frac{Fo}{3}\right) \quad (1)$$

Several methods to approximate two-dimensional irregular geometries to an elliptical model shape were investigated[2]. It was found that an approach based on using simple dimensional measurements resulted in the most accurate chilling time predictions across a set of 38 trials for seven irregular objects.

The long-term objective of the work was to develop a universal chilling time prediction method for convective cooling of solids of any shape. The last stage, which is the extension to three-dimensional irregular objects, is presented in this paper.

Model development

In the previous work with two-dimensional shapes[2], a key area was the definition of an equivalent shape for which predictions were made. While it would be expected that similar methodology to what had been successful for two-dimensional shapes might be suitable for three-dimensional shapes, it was still desirable to consider more than one possibility, especially as it was expected that two dimensional ratios (β_1 and β_2) would be needed.

Smith and co-workers[4–8] related irregular shapes to an equivalent ellipsoidal model shape that had equal orthogonal cross-sectional areas and the same characteristic

Nomenclature

A	Surface area (m^2)
Bi	Biot number $= hR/k$
c	Specific heat capacity (J kg^{-1} K^{-1})
D	Dimension (m)
E	Equivalent heat transfer dimensionality
Fo	Fourier number $= kt/(\rho cR^2)$
h	Heat transfer coefficient (W m^{-2} K^{-1})
k	Thermal conductivity (W m^{-1} K^{-1})
L	Lag factor or intercept
M	Dimensionless cooling rate
N	Number of heat transfer dimensions of an object or geometry
R	Object radius or half-thickness (m) $= D_1/2$
t	Chilling time (s)
T	Temperature (K or °C)
V	Volume (m^3)
Y	Fractional unaccomplished temperature change $= (T - T_a)/(T_i - T_a)$

Greek letters

α	First root of the transcendental equation for a sphere
β	Dimensional ratio
γ	Alternative dimensional ratio
λ	Alternative dimensional ratio
μ	Ratio of lag factors for mass-average and centre temperatures
ρ	Density (kg m^{-3})

Subscripts

0	For $Bi = 0$
1	Parameter 1
2	Parameter 2
3	Parameter 3
∞	For $Bi = \infty$
a	Cooling medium
c	Centre
exp	Experimental
FEM	Finite element calculation
i	Initial
m	Mass-average
x	Cross-sectional

dimension as those of the irregular shape that it replaced. The orthogonal cross-sections taken were the smallest and largest cross-sections that pass through the thermal centre and lie in the same plane as the characteristic dimension. For freezing, Cleland[9] and Hossain *et al.*[10] used an equivalent ellipsoid that has the same characteristic dimension R, the same smallest cross-sectional area through the thermal centre, A_x, and the same volume, V, as the irregular shape. They also investigated replacing the 'same volume' criterion with the 'same total surface area', but found that this led to inferior results.

In a similar manner to the investigation of two-dimensional shapes by the present authors[2] it was decided to investigate:

1. type of equivalent shape:
either use of an equivalent ellipsoid,
or use of an equivalent rectangular brick;
2. definition of dimensional ratios for the equivalent shape:
either use of an equal dimensional measurement approach to define the dimensional ratios β_1 and β_2 for the equivalent shape,
or use of a 'conservation' approach (of cross-sectional area and/or volume) in the irregular and equivalent shapes to define β_1 and β_2.

Of the two approaches for finding β_1 and β_2, the former has the advantage of real simplicity, involving a relatively simple single measurement in each direction. The latter requires more measurement: volume can be determined from mass and density, but cross-sectional area must be measured, and this can be difficult. Using conservation of volume and smallest cross-sectional area as the criteria, it follows that:

For the equivalent ellipsoid,

$$\beta_1 = \frac{A_x}{\pi R^2} \tag{2}$$

$$\beta_2 = \frac{3V}{4\pi R^3 \beta_1} \tag{3}$$

For the equivalent rectangular brick,

$$\beta_1 = \frac{A_x}{4R^2} \tag{4}$$

$$\beta_2 = \frac{V}{8R^3 \beta_1} \tag{5}$$

The four possible combinations of equivalent shape and measurement approach were designated as follows:

EA the equivalent ellipsoid model plus the conservation of area–volume approach;
EM the equivalent ellipsoid model plus the dimensional measurement approach;
BA the equivalent brick model plus the conservation of area–volume approach;
BM the equivalent brick model plus the dimensional measurement approach.

Development of expressions for E and L

The approach taken was to extend the previous formulae for E and L that applied to multidimensional regular shapes[1] and two-dimensional irregular shapes[2] to also encompass ellipsoids.

Formula for E

Data for E were generated as follows.

1. Plots of $\ln Y_c$ vs Fo for the ellipsoid shape were developed using calculations by the finite element method (FEM). A three dimensional finite element program was available[11], but the long computation and grid preparation times involved prevented large numbers

of calculations for fully three-dimensional grids. Therefore a two-dimensional axisymmetric implementation was used to enable two types of ellipsoid (the prolate spheroid, for which $\beta_1 = 1$, and the oblate spheroid, for which $\beta_1 = \beta_2$) to be studied in detail within a reasonable time frame.

2. Curve fitting of the plots was carried out by linear regression across the *Fo* ranges corresponding to $0.05 \leqslant Y_c \leqslant 0.7$.
3. The slopes of the plots were related to Equation (1) to estimate E.

Bi was varied logarithmically in nine even steps from 0.01 to 100; and β values in 13 logarithmically spaced steps from 1.0 to 10.0. This created a substantial database (but it did not cover all ellipsoidal shapes). The process was repeated for Y_m values but with curvefitting restricted to $0.05 \leqslant Y_m \leqslant 0.55$. Inspection of the E data generated in this manner suggested that the differences in E values calculated for Y_c and those calculated for Y_m were sufficiently small to be ignored. Therefore the E data derived from the calculations for the thermal centre were used in further analyses. Also determined from the linear regressions were values of the intercepts L_c and L_m for the lines that best fitted the FEM solutions.

As had been done for other shapes, the values that E should take at the two limiting conditions, $Bi = 0$ and $Bi \rightarrow \infty$, were investigated initially. These were denoted E_0 and E_∞ respectively.

At $Bi = 0$, E equals a dimensionless surface area to volume ratio AR/V[12]. However, calculation of the surface area of an ellipsoid is not straightforward, involving elliptical functions. Using an approximate formula for the surface area E_0 can be determined from

$$E_0 \approx \frac{2[\beta_1 + \beta_2 + \beta_1^2(1+\beta_2) + \beta_2^2(1+\beta_1)]}{2\beta_1\beta_2(1+\beta_1+\beta_2)} - \frac{[(\beta_1 - \beta_2)^2]^{0.4}}{15} \quad (6)$$

The error introduced by using this approximation is not greater than 3% for $1 < \beta_1 < 10$, $1 < \beta_2 < 10$[13].

As was the case for two-dimensional shapes[2], insights into expressions for E_∞ can be derived from considerations of the first term approximations to the series analytical solutions for various shapes. Details are given by Lin[13]. For example, for the rectangular brick (which is the intersection product of the analytical solutions for three infinite slabs of characteristic dimensions R, $\beta_1 R$ and $\beta_2 R$ respectively)

$$E_\infty = 0.75 + \frac{0.75}{\beta_1^2} + \frac{0.75}{\beta_1^2} \quad (7)$$

and for finite cylinders

$$E_\infty = 0.75 + \frac{1.01}{\beta_1^2} + \frac{0.75}{\beta_2^2} \quad (8)$$

By consideration of the numerically generated E data, and using analogies, the following equation for ellipsoids including the oblate and prolate spheroids was suggested:

$$E_\infty = 0.75 + \frac{1.01}{\beta_1^2} + \frac{1.24}{\beta_2^2} \quad (9)$$

As was the case for other shapes[1,2] a correction factor at intermediate β values was needed to develop the final expression for E_∞. When expressed in general form, applicable to all shapes, the equation for E_∞ became:

$$E_\infty = 0.75 + P_1 f(\beta_1) + P_2 f(\beta_2) \quad (10)$$

$$f(\beta) = \frac{1}{\beta^2} + 0.01 P_3 \exp\left(\beta - \frac{\beta^2}{6}\right) \quad (11)$$

Values of P_1, P_2 and P_3 for various geometries are stated in *Table 1*.

The weighting function used to determine E at intermediary *Bi* values from E_0 and E_∞ for other shapes[1,2] could also be applied to ellipsoids:

$$E = \frac{Bi^{4/3} + 1.85}{\dfrac{Bi^{4/3}}{E_\infty} + \dfrac{1.85}{E_0}} \quad (12)$$

Formula for L_c

In a similar fashion to that used for other shapes, data for L_c were subjected to non-linear regression analysis. Because a universal method applicable to all shapes was sought, this analysis concentrated on extending the previously published equations for other shapes. The resulting equations applicable to all shapes are

$$L_c = \frac{Bi^{1.35} + \dfrac{1}{\lambda}}{\dfrac{Bi^{1.35}}{L_\infty} + \dfrac{1}{\lambda}} \quad (13)$$

Table 1 Values of geometric parameters N, P_1, P_2, P_3, γ_1, γ_2 and λ for a variety of shapes

Tableau 1 *Valeurs des paramètres géométriques N, P_1, P_2, P_3, γ_1, γ_2 et λ pour plusieurs formes*

Shape	N	P_1	P_2	P_3	γ_1	γ_2	λ
Infinite slab ($\beta_1 = \beta_2 = \infty$)	1	0	0	0	∞	∞	1
Infinite rectangular rod ($\beta_1 \geqslant 1, \beta_2 = \infty$)	2	0.75	0	−1	$4\beta_1/\pi$	∞	γ_1
Brick ($\beta_1 \geqslant 1, \beta_2 \geqslant \beta_1$)	3	0.75	0.75	−1	$4\beta_1/\pi$	$1.5\,\beta_2$	γ_1
Infinite cylinder ($\beta_1 = 1, \beta_2 = \infty$)	2	1.01	0	0	1	∞	1
Infinite ellipse ($\beta_1 > 1, \beta_2 = \infty$)	2	1.01	0	1	β_1	∞	γ_1
Squat cylinder ($\beta_1 = \beta_2, \beta_1 \geqslant 1$)	3	1.01	0.75	−1	$1.225\,\beta_1$	$1.225\,\beta_2$	γ_1
Short cylinder ($\beta_1 = 1, \beta_2 \geqslant 1$)	3	1.01	0.75	−1	β_1	$1.5\,\beta_2$	γ_1
Sphere ($\beta_1 = \beta_2 = 1$)	3	1.01	1.24	0	1	1	1
Ellipsoid ($\beta_1 \geqslant 1, \beta_2 \geqslant \beta_1$)	3	1.01	1.24	1	β_1	β_2	γ_1

Table 2 Summary of percentage errors in predicted chilling times of spheroids to selected thermal centre temperatures comparing proposed method predictions with FEM predictions ($1 \leqslant \beta \leqslant 4$, $0.1 \leqslant Bi \leqslant 10, 0.05 \leqslant Y_c \leqslant 0.55$)

Tableau 2 *Résumé des erreurs de pourcentage pour des durées de réfrigération prévues de sphéroïdes à des températures du centre thermique choisies, et comparaison des prévisions par la méthode proposée et par les éléments finis (...)*

Shape	Mean	Std deviation	95% Confidence interval
Oblate spheroids	1.6	3.2	−5.4 to 7.6
Prolate spheroids	0.7	2.2	−4.6 to 4.1

where

$$L_\infty = 1.271 + 0.305\exp(0.172\gamma_1 - 0.115\gamma_1^2) + 0.425\exp(0.09\gamma_2 - 0.128\gamma_2^2) \quad (14)$$

Values of λ, γ_1 and γ_2 for various geometries are given in *Table 1*.

Formula for L_m

The approach taken for other shapes[1,2] could be directly applied. Expressed in a general form applicable to all shapes the equations are:

$$L_m = \mu L_c \quad (15)$$

where

$$\mu = \left(\frac{(1.5 + 0.69Bi)}{1.5 + Bi}\right)^N \quad (16)$$

N is the number of dimensions of an object in which heat transfer is significant; again, values are stated in *Table 1*.

The final prediction method was thus made applicable to objects of all shapes.

Testing of the new formulae for spheroids

Chilling times for the thermal centre and for the mass-average positions (t_c and t_m respectively) predicted by the proposed empirical method were tested against the FEM results discussed earlier. The calculated percentage errors in the times to reach certain thermal centre and mass-average temperatures are presented in *Tables 2* and *3*. The range of the percentage errors for the mass-average temperatures is larger than for the centre temperatures because the slope of the plot of ln Y_c vs Fo is slightly different from that of ln Y_m vs Fo (this was ignored in the above analysis, which used only centre temperatures to develop equations for E). There is some error in the curve-fit equations, but it is of the same order of magnitude as was achieved for regular and two-dimensional irregular shapes[1,2]. For most commonly encountered sets of conditions the error was less than about 5%. In the interests of maintaining algebraic simplicity this was accepted.

Table 3 Summary of percentage errors in predicted chilling times of spheroids to selected mass-average temperatures comparing proposed method predictions with FEM predictions ($1 \leqslant \beta \leqslant 4, 0.1 \leqslant Bi \leqslant 10$, Y_m corresponding to $0.05 \leqslant Y_c \leqslant 0.55$).

Tableau 3 *Résumé des erreurs de pourcentage pour des durées de réfrigération prévues de sphéroïdes à des températures moyennes choises, et comparaison des prévisions par la méthode proposée et par les éléments finis (...)*

Shape	Mean	Std deviation	95% Confidence interval
Oblate spheroids	2.1	3.5	−3.5 to 8.7
Prolate spheroids	−1.7	2.5	−8.3 to 2.0

Table 4 Mean thermal properties of chilling test materials (courtesy of the Meat Industry Research Institute of New Zealand)

Tableau 4 *Propriétés thermiques moyennes des matériaux expérimentaux utilisés pour les essais de réfrigération*

Material	ρ (kg m^{-3})	k (W m^{-1} K^{-1})	c (J kg^{-1} K^{-1})
Tylose (0°C to 30°C)	1028	0.50	3784
Cheddar cheese (−5°C to 20°C)	1055	0.31	3410

Experimental testing

Testing was carried out to investigate the various possibilities for relating irregular shapes to equivalent shapes, and to ascertain overall method accuracy. Details are given by Lin[13], so only a brief summary is presented here.

'Karlsruhe test substance'[14] or 'Tylose', a defined 23% (w/w) methylcellulose gel with well-characterized thermal properties similar to those of many high moisture foods, was used in some experiments. Because of its gel nature, Tylose is easily formed to different desired shapes, and is homogeneous once equilibration has occurred. However, because of its low rigidity, the Tylose gel can only be shaped into various geometries using moulds. Therefore it was not chosen for experimentation for three-dimensional irregular-shaped geometries with curved concave surfaces, for which moulds would be difficult to design and costly to make. Cheddar cheese, a real food of high homogeneity and isotropy, was chosen as an alternative test material for those experiments. One of the advantages of using Cheddar cheese is that it can be easily cut into any desired shape. Evaporative heat transfer was suppressed

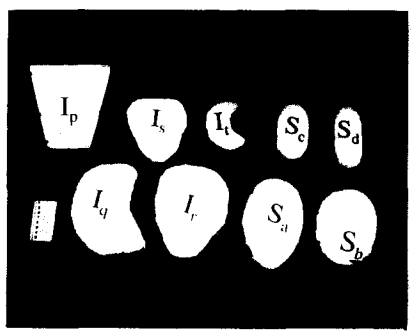

Figure 1 Three-dimensional test objects used in experimental work

Figure 1 *Objets expérimentaux tri-dimensionnels utilises dans l'expérience*

Table 5 Geometric parameters of three-dimensional test objects

Tableau 5 *Paramètres géométriques d'objets expérimentaux à trois dimensions*

	A_x (m^2)	V (m^3)	R (m)	β_1 (EM)	β_2 (EM)	β_1 (EA)	β_2 (EA)
I_p	0.010 148	0.001 297	0.0413	1.49	1.86	1.90	2.32
I_q	0.009 587	0.001 626	0.0500	1.22	1.83	1.22	2.55
I_r	0.012 715	0.001 699	0.0500	1.40	1.82	1.62	2.01
I_s	0.005 961	0.000 592	0.0250	2.50	2.68	3.04	2.98
I_t	0.002 322	0.000 273	0.0250	1.10	2.20	1.18	3.53
S_a	0.011 296	0.001 323	0.0560	1.09	1.39	1.15	1.57
S_b	0.008 931	0.001 147	0.0500	1.03	1.81	1.14	1.93
S_c	0.003 002	0.000 291	0.0250	1.40	2.42	1.53	2.91
S_d	0.002 625	0.000 301	0.0250	1.20	2.80	1.34	3.44

by thin plastic wraps. Thermal property data for both materials are stated in *Table 4*.

Nine different three-dimensional objects were investigated (*Figure 1*). They were divided into three groups according to their geometric configurations:

1. The mould of a frustrum of a square pyramid (I_p), which was constructed by Cleland *et al.*[15] was still available, and was used with Tylose as the test material.
2. Shapes S_a, S_b, S_c and S_d were quasi-ellipsoids, each of which was quite uniform in shape.
3. Shapes I_q, I_r, I_s and I_t were highly irregular, with I_q and I_t having concave surfaces.

Groups 2 and 3 were constructed from Cheddar cheese.

The pyramid shape was flat sided and could be accurately measured. For each of the Cheddar cheese samples, the three geometric dimensions were measured using a calliper. The characteristic dimension for each shape was calculated by halving the shortest dimension. The measurements were taken immediately prior to and after chilling processes and, in the case of the cheese samples, after dissection, when cross-sectional area measurements were also taken. No detectable differences were found between the various readings. The error in determining the geometric dimensions was considered to be less than ±2 mm for all the three-dimensional irregular shapes. The dimensional ratios found using two of the possible approaches for defining equivalent shapes are shown in *Table 5* for the nine three-dimensional samples.

All temperature measurements within the test objects were made using the same measurement equipment as had been used for two-dimensional shapes[2].

Both a brine immersion tank and an air blast tunnel were available as cooling systems. Only the air tunnel was used for experimentation on the Cheddar cheese samples but both were used for shape I_p.

A typical run involved the following steps:

1. The sample was held for 24 h at 30°C (Tylose) or 18°C (cheese) to establish a uniform initial temperature.
2. The cooling system was stabilized at its operating temperature of 0.5°C (Tylose runs) or −5°C (cheese runs).
3. Thermocouples were connected to the data logging system, and the samples were transferred to the sample rotation system in the cooling system. For cheese samples the sample holder was a wire mesh basket constructed of mesh that minimized contact between sample and wire. The pyramid was attached to the rotator via a single bolt placed in a part of the mould away from the thermal centre.

For the Tylose sample different *Bi*s were possible by using brine or air cooling or by adding insulating foam to the product surface. Neither of these options was possible for cheese, but some *Bi* variation was possible within limited ranges by varying sample size or air velocity. The latter approach would have added considerably to the cost of heat transfer coefficient measurement (see below). Further, the results for two-dimensional shapes[2] had shown that inaccuracy was not significantly correlated with *Bi*. It was therefore decided to use only a single air velocity of 2.0 m s^{-1} but a range of sample sizes, and to accept the limited range of *Bi* that would result.

The surface heat transfer coefficient for the irregular cheese shapes could not be measured directly without substantial difficulty. Seven rectangular bricks (of similar dimensions) were therefore constructed from the same kind of cheese and wrapped with plastic films in the same manner as for the irregular shapes. Seven separate chilling runs, one for each brick, were undertaken, and the heat transfer coefficient was back-calculated from the analytical solution for bricks[3] (*Table 6*). The differences in estimated h between runs were considered to be due largely to experimental error, so the mean h value was used for all the three-dimensional irregular cheese samples.

The pyramid shape in its plastic mould was chilled in three different heat transfer environments. The first case involved chilling in air. To determine h for this situation, runs using three differently shaped rectangular bricks

Table 6 Experimental measurements of heat transfer coefficient for Cheddar cheese bricks

Tableau 6 *Mesures expérimentales du coefficient de transfert de chaleur pour des briques de fromage de Cheddar*

Shape code and run number	$D_1 \times D_2 \times D_3$ (mm)	T_a (°C)	T_i (°C)	h (W m^{-2} K^{-1})
B_f	50 × 60 × 140	−5.4	18.2	24.0
B_g	50 × 70 × 121	−5.3	17.9	24.4
B_h	50 × 80 × 110	−5.4	18.2	26.9
B_i	112 × 122 × 155	−4.6	17.2	25.2
B_j	100 × 112 × 183	−4.5	18.6	24.3
B_k	100 × 141 × 181	−4.4	14.1	25.6
B_l	120 × 150 × 182	−5.3	13.5	24.7
		mean		25.0

Table 7 Experimental measurements of heat transfer coefficient in the air blast tunnel for Tylose bricks constructed of the same mould material as shape I_p

Tableau 7 *Mesures expérimentales du coefficient de transfert de chaleur dans un tunnel d'air soufflé pour des briques de Tylose construites avec le même matériau que la forme* I_p

Shape code and run number	$D_1 \times D_2 \times D_3$ (mm)	T_a (°C)	T_i (°C)	h (W m^{-2} K^{-1})
B_a21	104 × 125 × 152	0.7	31.8	17.4
B_a22	104 × 125 × 152	0.2	31.2	16.9
B_a23	104 × 125 × 152	0.3	31.3	19.0
B_b21	81 × 151 × 151	1.3	31.8	17.3
B_c21	54 × 127 × 201	1.3	31.5	18.1
B_c22	54 × 127 × 201	0.3	30.9	16.6
	mean			17.2

Table 8 Experimental data for chilling of three-dimensional irregular shapes

Tableau 8 *Données expérimentales de la réfrigération de formes irrégulières tri-dimensionnelles*

Shape code and run number	R (m)	h (W m^{-2} K^{-1})	T_a (°C)	T_i (°C)	M_{exp}	$L_{c\,exp}$
I_p1	0.0413	6.5	1.2	30.2	1.010	1.269
I_p2	0.0413	6.5	0.0	29.6	1.027	1.278
I_p3	0.0413	6.5	1.4	30.9	0.998	1.244
I_p4	0.0413	17.5	0.7	32.0	1.972	1.415
I_p5	0.0413	17.5	1.4	31.6	2.031	1.421
I_p6	0.0413	17.5	0.9	31.8	2.137	1.539
I_p7	0.0413	44.9	1.4	31.6	3.558	1.773
I_p8	0.0413	44.9	−0.1	31.4	3.428	1.903
I_p9	0.0413	44.9	−0.5	24.6	3.519	1.925
I_q1	0.0500	25.0	−4.1	14.7	4.189	1.607
I_f1	0.0500	25.0	−4.8	15.2	3.318	1.403
I_s1	0.0250	25.0	−5.3	18.4	1.747	1.320
I_s2	0.0250	25.0	−5.5	13.4	1.703	1.350
I_s3	0.0250	25.0	−5.4	13.2	1.826	1.374
I_t1	0.0250	25.0	−5.3	18.9	3.140	1.494
S_a1	0.0560	25.0	−4.6	15.5	5.015	1.621
S_a2	0.0560	25.0	−4.5	15.6	5.097	1.485
S_a3	0.0560	25.0	−4.4	15.0	4.711	1.520
S_b1	0.0500	25.0	−4.7	18.3	4.296	1.440
S_c1	0.0250	25.0	−5.5	16.0	2.244	1.330
S_d1	0.0250	25.0	−5.3	18.9	2.798	1.526

constructed of the same materials were used (*Table 7*). The second case involved chilling in the air tunnel with insulating foam present on the mould surface, and the third chilling in the brine tank. The h values for the latter two situations were estimated by summing relevant heat transfer resistances, which had been evaluated in earlier work[2]. Details are given by Lin[13].

Processing of experimental data

In total, 21 experiments were conducted with the three-dimensional irregularly shaped samples chosen for study. Orthogonal experimental designs in terms of Bi, Y, β_1 and β_2 were not feasible because of physical limitations in controlling the variables to preselected values. Also, a statistically based design was not essential, as no mathematical model building was undertaken from the results.

In presenting the experimental results, two derived parameters were calculated as follows:

1. Using thermal properties from *Table 4*, sample dimensions from *Table 5* plus the definitions of Y_c and Fo, the experimental data were converted to plots of $\ln Y_c$ vs Fo.
2. A best-fit line between $Y_c = 0.70$ and $Y_c = 0.05$ was found using linear regression of the following equation:

$$\ln Y_c = \ln(L_{c\,exp}) - M_{exp} Fo \tag{17}$$

where $L_{c\,exp}$ is the experimentally determined lag factor for the thermal centre, and M_{exp} is the experimentally determined dimensionless cooling rate.

The experimental results are given in *Table 8*. *Figure 2* shows a temperature–time profile at the thermal centre position for shape I_t that is typical of all the experimental runs.

Owing to the effort involved in grid preparation and limitations on computational time, finite element

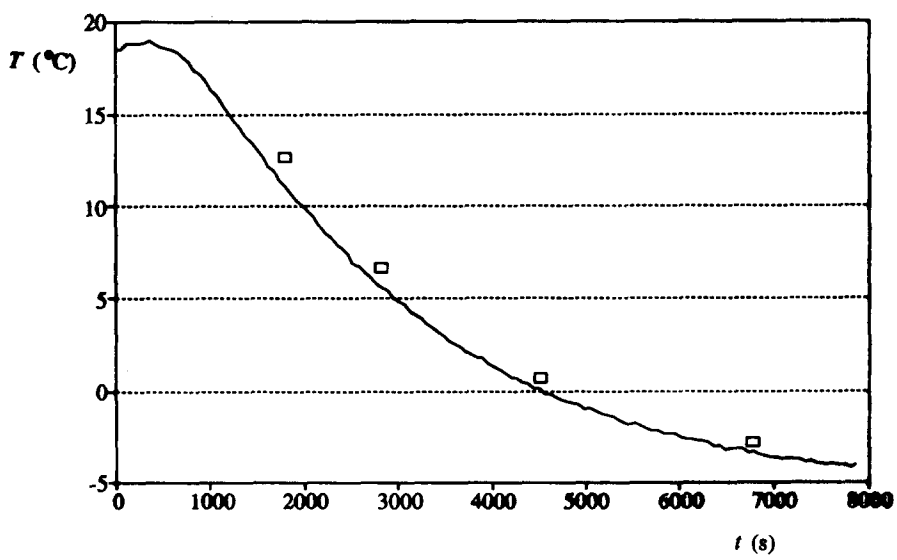

Figure 2 Centre temperature–time profile during chilling of the Cheddar cheese three-dimensional irregular shape I_t during Run I_t1: ——, experimental; □, predicted by the proposed method using approach EM to define the equivalent ellipsoid

Figure 2 *Profil température centrale-temps au cours de la réfrigération d'un objet* I_t *en forme de cheddar, irrégulier et tri-dimensionnel, au cours de l'essai* I_t1: ——, *expérimental;* □, *prévu par la méthode proposée utilisant l'approche EM pour définir l'ellipsoïde équivalente*

analysis was not carried out for the three-dimensional test samples.

Prediction accuracy of proposed method

The proposed calculation method was investigated in conjunction with the four geometric approaches defined earlier (EA, EM, BA, BM). The accuracy was quantified as the percentage difference between the chilling times for $Y_c = 0.50$, 0.25 and 0.10 predicted by the proposed method and the experimental value. The work with two-dimensional irregular shapes had suggested that EA and EM would be considerably more accurate than BA and BM[2]. This proved to be the case, so in *Table 9* only results for approaches EA and EM are reported. For the measured approach using the equivalent ellipsoidal model (EM), the mean percentage difference compared with measurements was low at 2.6%, whereas for the conservation of area–volume approach (EA), the mean difference was 9.9%. The 95% confidence interval of the percentage difference for the EM predictions compared with the experimentally measured chilling times was −6.4% to 11.6%.

Both the conservation of area–volume approach and the dimensional measurement approach still tend to overpredict measured data, especially at high Y_c values. Reasons for this were discussed in detail elsewhere[2]. In brief, the contribution effects of imprecise thermocouple placement (which affects predictions at all Y_c values) and non-linearity in the $\ln Y_c$ vs Fo plot (which affects predictions at high Y_c values) are primarily responsible.

The means and standard deviations were similar to those in the experiments for the two-dimensional irregular shapes[2]. The results therefore support the same conclusions as were reached for the two-dimensional work: that the EA approach for defining an equivalent ellipsoid is overly conservative, and that the EM approach is recommended.

No experimental tests of Y_m predictions were possible, owing to difficulty in measuring mass-average temperature. There is no reason to expect that the prediction accuracy of the proposed method for Y_m would be vastly different from that for Y_c. Nevertheless, for highly irregular shapes, especially those involving significant protrusions, prediction accuracy might deteriorate, as protrusions will contribute to some extent to mass-average temperature[2]. Experimental work would be difficult to carry out, but this is an area where there is potential for further study.

Summary of the proposed method for all geometric shapes

Combining the results of this paper with its two precursors[1,2], the complete procedure for application of the proposed method for predicting chilling rates is as follows:

1. Evaluation of the surface heat transfer coefficient (h).
2. Evaluation of the thermal properties of the object.
3. Measurement of the object dimensions D_1, D_2 and D_3:

D_1 = shortest dimension through the geometric centre of the object (first dimension);
D_2 = shortest dimension through the geometric centre of the object taken at right angles to the first dimension (second dimension);
D_3 = longest dimension through the geometric centre of the object taken as close as possible to right angles to both the first and second dimensions (third dimension).

For irregular shapes this implies approximation of the real shape to an equivalent infinite ellipse or ellipsoid. In using this measurement technique, protrusions are excised in the manner illustrated in Figure 4 of ref. 2.

4. Calculation of characteristic dimension R and two dimensional ratios β_1 and β_2:

$$R = \frac{D_1}{2} \qquad \beta_1 = \frac{D_2}{D_1} \qquad \beta_2 = \frac{D_3}{D_1}$$

5. Calculation of the Biot number (Bi).
6. Calculation of the equivalent heat transfer dimensionality at $Bi = 0$ (E_0) using:
   (a) ellipsoid or three-dimensional irregular shapes: Equation (6);

Table 9 Summary of percentage differences between experimental results and chilling times predicted by the proposed method for three-dimensional irregular shapes (M = mean, Sd = standard deviation)

Tableau 9 *Résumé des différences de pourcentage entre les résultats expérimentaux et les durées de réfrigération prévues par la méthode proposée, pour des formes irrégulières tri-dimensionnelles (M = moyenne; Sd = écart type)*

	$Y_c = 0.50$				$Y_c = 0.25$				$Y_c = 0.10$				Cumulative Results			
Approach	EA		EM		EA		EM		EA		EM		EA		EM	
Shape	M	Sd	M	Sd	M	Sd	M	Sd	M	Sd	M	Sd	M	Sd	M	Sd
S_a	15.5	–	9.3	–	9.9	–	3.5	–	3.5	–	−3.4	–	9.6	–	3.1	–
S_b	17.2	–	12.1	–	10.9	–	6.6	–	4.0	–	−2.0	–	10.7	–	5.6	–
S_c	9.3	–	3.8	–	3.3	–	−2.7	–	2.6	–	−4.0	–	5.1	–	−1.0	–
S_d	8.0	–	2.2	–	9.8	–	3.3	–	12.9	–	5.3	–	10.2	–	3.6	–
S group	12.5	5.3	6.9	4.7	8.5	3.4	2.7	3.4	5.8	3.6	−1.0	3.2	8.9	5.4	2.8	5.4
I_p	15.1	3.9	0.5	3.0	13.9	2.9	−0.2	2.1	15.0	2.6	1.2	2.7	14.7	3.2	0.5	2.7
I_q	15.7	–	5.8	–	11.8	–	1.7	–	11.5	–	0.5	–	13.0	–	2.7	–
I_r	16.7	–	8.1	–	9.3	–	1.7	–	3.4	–	−4.3	–	9.8	–	1.8	–
I_s	3.6	–	2.4	–	−0.2	–	−2.6	–	−0.9	–	−4.0	–	0.8	–	−1.4	–
I_t	14.3	–	9.2	–	14.6	–	7.8	–	17.1	–	8.0	–	15.3	–	8.3	–
I group	13.1	5.7	5.2	3.8	9.9	6.2	1.7	3.3	9.2	7.4	0.3	4.3	10.7	6.6	2.4	4.0
Overall	12.8	5.6	5.9	4.7	9.2	5.6	2.1	3.6	7.7	7.1	−0.3	4.1	9.9	6.3	2.6	4.5

(b) ellipse or two-dimensional irregular shapes:

$$E_0 = \left(1 + \frac{1}{\beta_1}\right)\left[1 + \left(\frac{\beta_1 - 1}{2\beta_1 + 2}\right)^2\right] \quad (18)$$

(c) finite cylinders, bricks, infinite rectangular rods:

$$E_0 = 1 + \frac{1}{\beta_1} + \frac{1}{\beta_2} \quad (19)$$

(d) sphere ($E_0 = 3$), infinite cylinder ($E_0 = 2$), infinite slab ($E_0 = 1$).

7. Calculation of the equivalent heat transfer dimensionality at $Bi = \infty(E_\infty)$ using Equations (10) and (11) in combination with *Table 1*.

8. Calculation of the equivalent heat transfer dimensionality (E) using Equation (12).

9. Calculation of the lag factor at $Bi = \infty(L_\infty)$ using Equation (14) in combination with *Table 1*.

10. Calculation of the alternative dimensional ratio (λ) using the expressions given in *Table 1*.

11a. Calculation of the lag factor for thermal centre positions (L_c) using Equation (13).

11b. Calculation of the lag factor for mass-average situations (L_m) using Equation (15), noting that this step is required only for calculations related to mass-average conditions.

12. Calculation of the first root of the transcendental equation for a sphere (α):

$$\alpha \cot \alpha + Bi - 1 = 0 \quad (20)$$

13. Calculation of the chilling time to achieve a desired temperature (t_c or t_m) or temperature reached after a defined chilling time (T_c or T_m):

For thermal centre:

$$t_c = \frac{3\rho c R^2}{\alpha^2 k E} \ln\left(\frac{T_i - T_a}{T_c - T_a} L_c\right) \quad (21)$$

or

$$T_c = L_c \exp\left(-\frac{k E t_c \alpha^2}{3\rho c R^2}\right)(T_i - T_a) + T_a \quad (22)$$

For mass-average:

$$t_m = \frac{3\rho c R^2}{\alpha^2 k E} \ln\left(\frac{T_i - T_a}{T_m - T_a} L_m\right) \quad (23)$$

or

$$T_m = L_m \exp\left(-\frac{k E t_m \alpha^2}{3\rho c R^2}\right)(T_i - T_a) + T_a \quad (24)$$

14. Checking of the range of fractional unaccomplished temperature change (Y). If $Y_c > 0.7$ or $Y_m > 0.55$, results calculated using the prediction method may be unreliable.

Conclusions

The experimental results suggest the use of the ellipsoid rather than the rectangular brick as the appropriate equivalent model shape for three-dimensional irregular geometries.

To define the equivalent ellipsoid, the dimensional ratios β_1 and β_2 should be based on measured dimensions. As well as best accuracy, this approach has the advantage that it is consistent with the manner in which geometries were defined for the regular geometries.

Using the equivalent ellipsoid based on measured dimensions approach, the proposed chilling time prediction method performs satisfactorily. Lack of fit is probably due more to experimental error than to errors in the form of geometric approximation and the prediction method itself.

References

1 **Lin, Z., Cleland, A. C., Cleland, D. J., Serrallach, G. F.** Prediction of chilling times for objects of regular multi-dimensional shapes using a general geometric factor *Refrig Sci Technol Proc* (1993) 259–267

2 **Lin, Z., Cleland, A. C., Cleland, D. J., Serrallach, G. F.** A simple method for prediction of chilling times for objects of two-dimensional irregular shapes *Int J Refrig* (1996) **19** 95–106

3 **Carslaw, H. S., Jaeger, J. C.** *Conduction of Heat in Solids* 2nd edn, Clarendon Press, Oxford (1959)

4 **Smith, R. E., Nelson, G. L., Henrichson, R. L.** Analyses on transient heat transfer from anomalous shapes *Trans ASAE* (1967) **10** 236–245

5 **Smith, R. E., Nelson, G. L., Henrichson, R. L.** Applications of geometry analysis of anomalous shapes to problems in transient heat transfer *Trans ASAE* (1968) **11** 296–302

6 **Clary, B. L., Nelson, G. L., Smith, R. E.** Heat transfer from hams during freezing by low temperature air *Trans ASAE* (1968) **11** 496–499

7 **Smith, R. E., Nelson, G. L.** Transient heat transfer in solids: theory versus experimental *Trans ASAE* (1969) **12** 833–836, 844

8 **Clary, B. L., Nelson, G. L., Smith, R. E.** Applications of geometry analysis technique in determining the heat transfer rates from biological materials *Trans ASAE* (1971) **14** 586–589

9 **Cleland, D. J.** Prediction of freezing and thawing times for foods *PhD Thesis* Massey University, New Zealand (1985)

10 **Hossain, Md. M., Cleland, D. J., Cleland, A. C.** Prediction of freezing and thawing times for foods of three-dimensional irregular shape by using a semi-analytical geometric factor *Int J Refrig* (1992) **15** 241–246

11 **Cleland, D. J., Cleland, A. C., Earle, R. L., Byrne, S. J.** Prediction of freezing and thawing times for multi-dimensional shapes by numerical methods *Int J Refrig* (1987) **10** 32–39

12 **Cleland, A. C.** *Food Refrigeration Processes–Analysis, Design and Simulation* Elsevier Applied Science, London and New York (1990)

13 **Lin, Z.** Prediction of chilling times of foods *PhD Thesis* Massey University, New Zealand (1994)

14 **Riedel, L.** Eine prufsubstanz fur gefrierversuche *Kaltetechnik* (1960) **12** 222–226

15 **Cleland, D. J., Cleland, A. C., Earle, R. L., Byrne, S. J.** Experimental data for freezing and thawing of multi-dimensional objects *Int J Refrig* (1987) **10** 22–31